J. Fluid Mech. (1981), *vol.* 103, *pp.* 161–182
Printed in Great Britain

A Reynolds-stress closure model of turbulence applied to the calculation of a highly curved mixing layer

By M. M. GIBSON
Mechanical Engineering Department, Imperial College, London

AND W. RODI
Sonderforschungsbereich 80, University of Karlsruhe, Germany

(Received 11 June 1979 and in revised form 23 March 1980)

The measurements in a highly curved mixing layer reported by Castro & Bradshaw (1976) are used to evaluate the performance of a calculation method based on the solution of modelled transport equations for the Reynolds stresses and the dissipation rate of turbulent energy. The model reproduces the suppression of turbulence by stabilizing curvature and, downstream of the curved region, where the flow returns asymptotically to being a plane mixing layer, calculated values of turbulent intensity and shear stress overshoot the plane-layer values in accordance with the experimental observations. The results are compared with those obtained by Townsend (1980) from a rapid-distortion model which correctly predicts the streamwise variation of the shear stress to intensity ratio. By contrast, calculations based on a conventional two-equation eddy-viscosity model fail badly to account for curvature effects on this flow.

1. Introduction

As part of a general investigation of complex turbulent flows Castro & Bradshaw (1976) – referred to throughout this paper as CB – report extensive one-point measurements in a highly-curved mixing layer. The object of the experiment was 'to document the effect of complicating influences so that some of the calculation methods which have proved satisfactory in simple shear layers can be extended with some confidence to complex flows'. In the present paper we use these measurements to assess the performance of a calculation method based on the solution of modelled transport equations for the Reynolds stresses.

The presence in curved shear layers of the 'complicating influences' referred to by CB has long been recognized, although they are not yet fully understood physically and their representation in calculation methods has been only partially successful. The principal observed effect of streamline curvature on a shear layer is to diminish the turbulent intensity and shear stress when the angular momentum of the mean-flow increases with increasing radius of curvature and to increase these quantities in the opposite situation. For a full discussion of these effects and a review of previous work the reader is referred to CB and to the comprehensive survey paper by Bradshaw (1973). In the present paper only the CB data are considered. Apart from some earlier, much less detailed, measurements reported by Wyngaard *et al.* (1968) they are the only results reported for a *free* curved shear layer.

0022-1120/81/4617-2900 $02.00

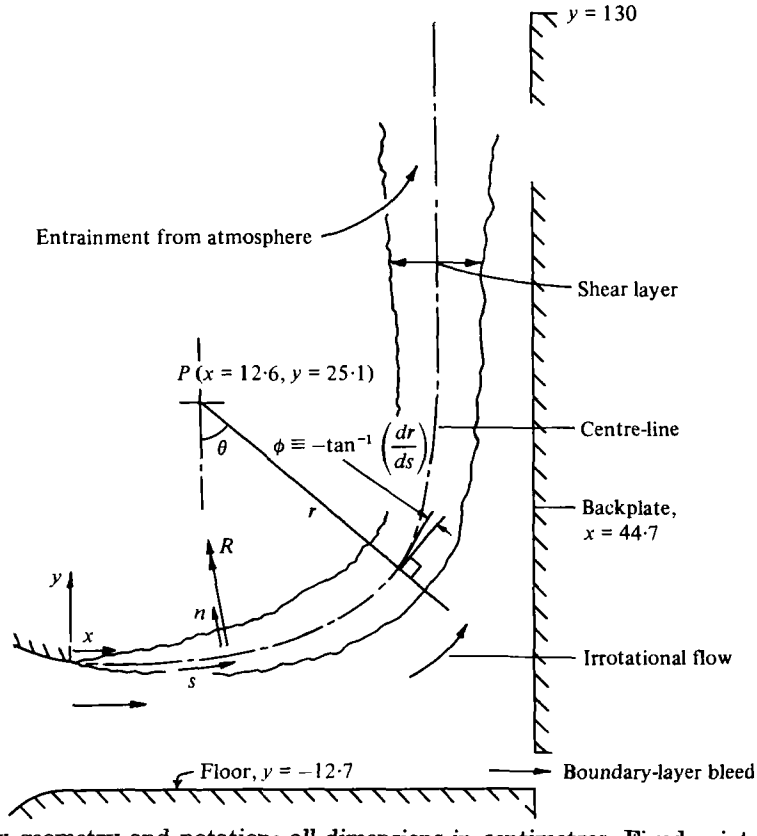

FIGURE 1. Flow geometry and notation: all dimensions in centimetres. Fixed point P is near, but not at, centre of curvature: the latter varies with s. (Reproduced from Castro & Bradshaw (1976) by permission of the authors and the Cambridge University Press.)

The configuration chosen by CB for their experiments is shown in figure 1 which is reproduced (by permission) from the original paper. The measurements were made in the mixing layer bounding a plane jet with an irrotational core impinging normally on a backplate set 44·7 cm from the nozzle. The flow can be thought of as half a two-dimensional impinging jet with a potential core and with the 'floor' replacing the symmetry plane. The sense of the curvature is stabilizing (i.e. turbulence is depressed in the mixing layer) and the ratio of shear-layer thickness to streamline radius of curvature reaches a maximum of about 0·2. Downstream of the impingement region the shear layer returns asymptotically to being a classical plane mixing layer. The most spectacular feature of the measurements reported by CB is that the Reynolds stresses and other turbulent quantities, after decreasing as expected in the region of high stabilizing curvature, rise rapidly further downstream and overshoot the plane-layer values before finally decreasing. The results are considered by CB to 'undermine many of the principles used in current calculation methods for shear layers, such as the automatic use of the shear-layer thickness to provide a length scale, the rotational invariance of turbulence models based on second-order transport equations, and the gradient diffusion hypothesis for turbulent transport'.

In a recent paper by Townsend (1980) the rapid-distortion approximation is used

to predict the streamwise variation of $\overline{uv}/\overline{q^2}$ in the CB flow. The author argues that, while the Reynolds-stress equations are exact, they can say very little about the flow patterns and in particular about the form and orientations of the energy-containing eddies. The curved mixing layer is cited as an example of unusual flow distortion for which Reynolds-stress methods will not give correct results because the distortion is considered to be so complex that its history over the lifetime of an eddy must be accounted for. We shall return to this point later to show that, in the CB flow, these effects do not preclude modelling in terms of the local strain rate. The observed behaviour of the structure parameter, $\overline{uv}/\overline{q^2}$, which Townsend uses to support his argument can, in fact, be ascribed directly to local changes in the extra strain due to curvature which are accounted for in the Reynolds-stress equation. In its present form the rapid-distortion model sets out only to predict stress ratios and, if it were to form part of a calculation scheme, another equation would be needed to determine intensities. Methods based on modelled transport equations for the Reynolds-stresses are capable of providing this information and the main purpose of the present study is to establish whether the applicability of such a method is in fact limited by the effects described by Townsend.

Considerable progress has been made in developing 'Reynolds-stress models' of turbulence, and numerous proposals for closing the set of transport equations have appeared in the literature. A method which gives good results for simple shear layers, and which has also been used successfully to calculate more complicated flows, is that developed by Launder, Reece & Rodi (1975) (afterwards cited as LRR) from earlier work by Hanjalic & Launder (1972). Two applications in particular may be cited here: the calculation of curved wall flows and of a curved free jet by Irwin & Smith (1975) and the prediction of the effects of buoyancy on shear-layer turbulence by Gibson & Launder (1976, 1978) where there is a well-known analogy with streamline curvature (Bradshaw 1969). In a study of curved wall flow Mellor (1975) has also shown that a different Reynolds-stress closure method accounts fairly well for the observed extinction of shear stress by strong stabilizing curvature. Unfortunately, like Irwin & Smith, Mellor was unable to make very detailed comparisons with measurements of turbulence quantities and some of the more interesting features of the CB results did not appear in the wall-flow data used by these authors. The turbulence model developed by Launder and his collaborators forms the basis of the present study, although we have made use of later recommendations for the model constants. Its most important feature is the treatment of pressure-strain redistribution in the transport equations for the Reynolds stresses. The main contribution in the present work is the adaptation of this treatment so as to include the effects of extra strain due to streamline curvature, and a demonstration that many of the curvature effects observed by CB can be accounted for.

The remainder of the paper consists of a brief description of the modelled Reynolds-stress equations for curved flow, the calculation procedure and a detailed comparison of the calculated results with the turbulence measurements reported by CB. The overall performance of the calculation method is assessed in a concluding section which also contains a brief discussion of the calculation method in relation to Townsends (1980) rapid-distortion model.

2. The turbulence model

2.1. *The Reynolds-stress equations*

The transport equations for Reynolds stress in a fairly thin, curved, shear layer are most conveniently expressed in the s-n co-ordinate system described by Bradshaw (1973) and used also by CB. The co-ordinates are shown in figure 1: s is distance measured along an arbitrarily chosen curved centreline with local radius of curvature R, and n is measured along straight lines normal to the centreline and toward the centre of curvature. The third co-ordinate, z, is measured along straight lines normal to the s-n plane. U, V and W are the components of mean velocity in the s, n and z directions and u, v and w the corresponding fluctuating components. As a consequence of these definitions R is negative throughout the flow and the Reynolds shear stress, $\overline{uv}$, is generally positive. For constant R the system reduces to polar co-ordinates (r, θ, z) with $r \equiv n + R$ and $\theta \equiv s/R$.

The Reynolds number is assumed to be high enough for the fine-scale turbulent motion to be isotropic and viscous diffusion to be negligibly small. The turbulent-energy dissipation rate, ϵ, is then distributed equally among components $\overline{u^2}$, $\overline{v^2}$, $\overline{w^2}$ and all the viscous terms disappear from the $\overline{uv}$ equation. With these assumptions the transport equations for the Reynolds stresses in a two-dimensional shear layer are:

$$\frac{D}{Dt}(\tfrac{1}{2}\overline{u^2}) = -\overline{u^2}\left(\frac{\partial U}{\partial s}+\frac{V}{R}\right)-\overline{uv}\left[\left(1+\frac{n}{R}\right)\frac{\partial U}{\partial n}-\frac{U}{R}\right]$$
$$-2\overline{uv}\frac{U}{R}-\frac{\partial}{\partial s}\left(\frac{\overline{p'u}}{\rho}+\tfrac{1}{2}\overline{u^3}\right)-\frac{\partial}{\partial n}\left[\left(1+\frac{n}{R}\right)(\tfrac{1}{2}\overline{u^2v})\right]-\frac{\overline{u^2v}}{R}+\frac{\overline{p'}\,\overline{\partial u}}{\rho\,\partial s}-\tfrac{1}{3}\epsilon, \tag{1}$$

$$\frac{D}{Dt}(\tfrac{1}{2}\overline{v^2}) = -\overline{v^2}\left(1+\frac{n}{R}\right)\frac{\partial V}{\partial n}-\overline{uv}\frac{\partial V}{\partial s}+2\overline{uv}\frac{U}{R}-\frac{\partial}{\partial s}(\tfrac{1}{2}\overline{uv^2})$$
$$-\frac{\partial}{\partial n}\left[\left(1+\frac{n}{R}\right)\left(\frac{\overline{p'v}}{\rho}+\tfrac{1}{2}\overline{v^3}\right)\right]+\frac{\overline{u^2v}}{R}+\frac{\overline{p'}}{\rho}\frac{\partial}{\partial n}\left[\left(1+\frac{n}{R}\right)v\right]-\tfrac{1}{3}\epsilon, \tag{2}$$

$$\frac{D}{Dt}(\tfrac{1}{2}\overline{w^2}) = -\frac{\partial}{\partial s}(\tfrac{1}{2}\overline{uw^2})-\frac{\partial}{\partial n}\left[\left(1+\frac{n}{R}\right)(\tfrac{1}{2}\overline{vw^2})\right]+\frac{\overline{p'}\,\overline{\partial w}}{\rho\,\partial z}-\tfrac{1}{3}\epsilon, \tag{3}$$

$$\frac{D}{Dt}(\overline{uv}) = -\overline{u^2}\frac{\partial V}{\partial s}-\overline{v^2}\left[\left(1+\frac{n}{R}\right)\frac{\partial U}{\partial n}-\frac{U}{R}\right]+2(\overline{u^2}-\overline{v^2})\frac{U}{R}-\frac{\partial}{\partial s}\left(\frac{\overline{p'v}}{\rho}+\overline{u^2v}\right)$$
$$-\left(1+\frac{n}{R}\right)\frac{\partial}{\partial n}\left(\frac{\overline{p'u}}{\rho}+\overline{uv^2}\right)-\frac{2\overline{uv^2}-\overline{u^3}}{R}+\overline{\frac{p'}{\rho}\left[\frac{\partial v}{\partial s}+\left(1+\frac{n}{R}\right)\frac{\partial u}{\partial n}\right]}. \tag{4}$$

The dominant terms in each equation are underlined.

The left-hand sides of the equations represent transport by the mean flow where

$$\frac{D}{Dt} \equiv U\frac{\partial}{\partial s}+\left(1+\frac{n}{R}\right)V\frac{\partial}{\partial n}.$$

The terms on the right-hand sides of (1)–(3) represent generation, turbulent transport, pressure-strain redistribution (in which p' is the fluctuation in static pressure) and viscous dissipation. The equivalent terms appear in the shear-stress equation but there is negligible viscous dissipation of $\overline{uv}$ at high Reynolds number.

Summation of equations (1)–(3) produces the transport equation for turbulent energy, $\frac{1}{2}\overline{q^2}$, given by CB:

$$\underline{\frac{D}{Dt}(\tfrac{1}{2}\overline{q^2})} = -\overline{u^2}\left(\frac{\partial U}{\partial s}+\frac{V}{R}\right)-\overline{v^2}\left(1+\frac{n}{R}\right)\frac{\partial V}{\partial n}-\underline{\overline{uv}\left[\left(1+\frac{n}{R}\right)\frac{\partial U}{\partial n}-\frac{U}{R}+\frac{\partial V}{\partial s}\right]}$$
$$-\frac{\partial}{\partial s}\left(\frac{\overline{p'u}}{\rho}+\tfrac{1}{2}\overline{uq^2}\right)-\frac{\partial}{\partial n}\left[\left(1+\frac{n}{R}\right)\underline{\left(\frac{\overline{p'v}}{\rho}+\tfrac{1}{2}\overline{vq^2}\right)}\right]-\underline{\epsilon}, \tag{5}$$

where the terms on the right represent production, turbulent transport (diffusion) and dissipation, ϵ. If only the underlined (dominant) terms are considered the production of $\frac{1}{2}\overline{q^2}$ is $-\overline{uv}[(1+n/R)\partial U/\partial n - U/R]$ which has the form (turbulent shear stress) × (rate of strain of mean flow). In the case of a simple shear layer energy is generated from this source solely in the streamwise component $\overline{u^2}$. For a curved shear layer additional sources $\pm\overline{uv}\,U/R$ appear in the equations for $\overline{u^2}$ and $\overline{v^2}$. These have the form (shear stress) × (extra strain rate due to curvature) and have the effect of transferring energy from the cross-stream to the streamwise component when the sense of the curvature is stabilizing.

The mean-flow transport and generation terms in (1)–(4) are expressed in terms of known quantities in a calculation scheme. Closure approximations are required for the turbulent transport and pressure-strain redistribution terms. It is then possible to solve the stress equations (1)–(4) numerically together with the momentum and continuity equations of the mean flow and a modelled transport equation for the dissipation rate ϵ.

2.2. *Treatment of the pressure-strain correlations*

It is now generally accepted that, as first pointed out by Rotta (1951), the pressure-strain redistribution terms in the Reynolds-stress equations consist of: (*a*) turbulence interactions tending to equalize the turbulent energy in each component and (*b*) interactions of the turbulence field with the strain rate of the mean flow. These interactions are modelled by the following simple expression, 'Model 2' in LRR, written in Cartesian tensor notation for brevity:

$$\overline{\frac{p'}{\rho}\left(\frac{\partial u_i}{\partial x_j}+\frac{\partial u_j}{\partial x_i}\right)} = \underbrace{-C_1\frac{\epsilon}{\frac{1}{2}\overline{q^2}}(\overline{u_iu_j}-\tfrac{1}{3}\delta_{ij}\overline{q^2})}_{\pi_{ij,1}}\underbrace{-C_2(P_{ij}-\tfrac{2}{3}\delta_{ij}P)}_{\pi_{ij,2}}, \tag{6}$$

where P_{ij} and P are the rates of production of $\overline{u_iu_j}$ and $\frac{1}{2}\overline{q^2}$ respectively and the coefficients C_1 and C_2 are supposed constants in high-Reynolds-number turbulence.

The term $\pi_{ij,1}$ represents the turbulence contribution to pressure strain and is due to Rotta (1951). It is based on the hypothesis that in flows with negligible mean strain the rate of return of anisotropic turbulence to isotropy is proportional to the level of anisotropy. The characteristic decay time is taken here as $\frac{1}{2}\overline{q^2}/\epsilon$. The second term, $\pi_{ij,2}$, which accounts for the mean-strain effects, was proposed by Naot *et al.* (1970) as a replacement for Rotta's expression, and by Reynolds (1970). LRR identified this term as the dominant one in a more general expression and combined it with $\pi_{ij,1}$ as in (6) to obtain good results for a number of simple, free, shear layers. Additional support for the use of (6) is provided by the recent study by Leslie (1980) of homogeneous shear flow which shows that this relatively simple treatment of pressure

strain produces better results for this type of flow than does the more elaborate 'Model 1' of LRR.

Strictly speaking the mean-strain component $\pi_{ij,2}$ depends not only on the local rate of strain as it is modelled in (6) but on the entire strain field about the point considered. However for the error involved in this approximation to be significant the strain would have to be so non-homogeneous as to vary significantly over distances comparable with the integral scale of the turbulence. If this is taken as $0{\cdot}1(\overline{q^2})^{\frac{3}{2}}/\epsilon$ (where the coefficient 0·1 is chosen (Rotta 1951) so that the scale corresponds to that of the lateral velocity correlation in isotropic turbulence) the data show a variation of roughly 0·02 times the streamwise distance s. The variation of the extra strain U/r associated with curvature nowhere exceeds 5% over this length. Following Rotta (1951) the error introduced in the model for $\pi_{ij,2}$ by assuming the strain to be homogeneous may be estimated by expressing the strain field in terms of a Taylor-series expansion about the point considered. For homogeneous turbulence the first term containing the streamwise variation of extra strain is the second derivative $\partial^2(U/r)/\partial s^2$. Using Rotta's relations, strictly valid only for isotropic turbulence, the maximum error arising from the neglect of this contribution, which occurs at the point of maximum curvature, is estimated as less than 2%. The use of a local strain in (6) would therefore appear to be justified for this flow. It is also worth noting that for weak homogeneous distortion of turbulence which is initially isotropic the expression (6) for $\pi_{ij,2}$ is identical to the result obtained from the rapid-distortion theory when, as here, the coefficient C_2 is set equal to 0·6.

In adapting (6) to curved flow, no distinction has been drawn between mean-shear production and that due to extra strain or rotation of the axes. Thus, in the $\frac{1}{2}\overline{u^2}$ equation (1), P_{11} is taken as the total production rate $-\overline{uv}[(1+n/R)\partial U/\partial n + U/R]$ which has the form (shear stress) × (vorticity of mean flow), and the shear-stress production term P_{12} includes $2(\overline{u^2}-\overline{v^2})U/R$. Only the principal (underlined) production terms are used in modelling the pressure strain to give the expressions which are set out in full in table 1.

The model constants C_1 and C_2 are assigned values recently recommended by Gibson & Launder (1978). C_2 takes the value 0·6, as in LRR, required to satisfy (6) for the case of isotropic turbulence subjected to sudden distortion. C_1 is set equal to 1·8 (instead of 1·5 in LRR or 2·5 in Hanjalic & Launder (1972))† to improve the dicted level of shear stress in plane free shear flow.

2.3. *The remaining closure approximations*

Turbulent transport of Reynolds stress is approximated by the simple gradient-diffusion hypothesis for the triple correlations due, originally, to Daly & Harlow (1970) and written here, for brevity, in Cartesian-tensor notation:

$$-\overline{u_i u_j u_k} = C_t \frac{\overline{q^2}}{2\epsilon} \overline{u_k u_l} \frac{\partial \overline{u_i u_j}}{\partial x_l}. \tag{7}$$

Equation (7) is not compatible in its symmetry properties since only the left-hand side is independent of the order of the indices i, j and k. However, LRR found that it produced satisfactory results for most free shear flows and that the results given by a

† It should be noted that these two values were initially chosen to suit different pressure-strain models.

rotationally-invariant form were not supported by the experimental evidence. Lumley (1980) has suggested that this might be due to the absorption in (7) of some pressure diffusion which is not symmetrical and which is not modelled explicitly. It will be seen later that (7) underestimates turbulent transport of Reynolds stress in a plane-mixing layer and that the behaviour observed by CB in the curved flow is so complicated that it cannot possibly be described by such a simple relationship. Nevertheless we have preferred to retain this formulation, with the value of C_t which gives the best results for a number of different flows, rather than to introduce *ad hoc* modifications for curvature at this stage. The coefficient C_t is set equal to 0·22† and the effects of curvature are expressed indirectly through changes in the stress levels, and particularly that of $\overline{v^2}$, since for the shear layer where cross-stream transport predominates, (7) reduces to:

$$-\overline{vu_iu_j} = C_t \frac{\overline{q^2}}{\epsilon} \overline{v^2} \frac{\partial \overline{u_iu_j}}{\partial n}. \tag{8}$$

The triple-correlation terms explicitly associated with curvature are omitted at this level of approximation and are, in any case, found by Castro (1973) to be very small.

The turbulent-energy dissipation rate, ϵ, is obtained from the model transport equation used by LRR. The high Reynolds-number form for curved flow is expressed in s-n co-ordinates as

$$\frac{D\epsilon}{Dt} = C_\epsilon \frac{\partial}{\partial n}\left[\left(1+\frac{n}{R}\right)\frac{\overline{q^2}}{2\epsilon}\overline{v^2}\frac{\partial \epsilon}{\partial n}\right] + \frac{\epsilon^2}{\frac{1}{2}\overline{q^2}}\left(C_{\epsilon_1}\frac{P}{\epsilon} - C_{\epsilon_2}\right). \tag{9}$$

Turbulent transport of ϵ is here approximated by an expression similar in form to (8). The rates of generation and destruction of ϵ are assumed individually to be proportional to those of turbulent energy so that curvature effects appear through the definition of P:

$$P \equiv -\overline{uv}\left[\left(1+\frac{n}{R}\right)\frac{\partial U}{\partial n} - \frac{U}{R}\right]. \tag{10}$$

The coefficients C_ϵ, C_{ϵ_1}, C_{ϵ_2} are taken as 0·18, 1·45 and 1·90 as recommended by Launder & Morse (1979). These values differ slightly from the original recommendations of LRR (0·15, 1·44, 1·90) but have been preferred simply because they are the result of later work.

It may be of interest at this stage to note briefly the implications of rapid-distortion theory in relation to the terms in the Reynolds-stress equations. The rapid-distortion theory reviewed by Hunt (1978) neglects gradients of the triple velocity correlation (turbulent diffusion), the turbulence contribution to pressure strain, $\pi_{ij,1}$, and usually also the energy dissipation rate. The mean-strain part of the pressure-strain correlation, $\pi_{ij,2}$, and pressure diffusion are calculated directly from linearized versions of the equations of motion. As noted above, the present model for $\pi_{ij,2}$ is consistent with the result of rapid-distortion theory for isotropic turbulence subjected to sudden distortion.

† Launder & Morse (1979) note that the value 0·25 in LRR was published in error for 0·21. The value 0·22, and the remaining model constants of this section, have been arrived at by Morse (1979) from a later independent optimisation study.

Quantity	Mean-flow transport	Turbulent transport (diffusion)	Generation	Destruction	Pressure-strain redistribution
$\frac{1}{2}\overline{u^2}$	$\frac{D}{Dt}(\frac{1}{2}\overline{u^2})$	$C_t\frac{\partial}{\partial n}\left(h\frac{\overline{q^2}}{2\epsilon}\overline{v^2}\frac{\partial\overline{u^2}}{\partial n}\right)$	$-\overline{uv}\left(h\frac{\partial U}{\partial n}-\frac{U}{R}\right)-2\overline{uv}\frac{U}{R}$	$-\frac{1}{3}\epsilon$	$-C_1\frac{\epsilon}{\frac{1}{2}\overline{q^2}}(\overline{u^2}-\frac{1}{3}\overline{q^2})+\frac{2}{3}C_2\,\overline{uv}\left(h\frac{\partial U}{\partial n}+2\frac{U}{R}\right)$
$\frac{1}{2}\overline{v^2}$	$\frac{D}{Dt}(\frac{1}{2}\overline{v^2})$	$C_t\frac{\partial}{\partial n}\left(h\frac{\overline{q^2}}{2\epsilon}\overline{v^2}\frac{\partial\overline{v^2}}{\partial n}\right)$	$2\,\overline{uv}\frac{U}{R}$	$-\frac{1}{3}\epsilon$	$-C_1\frac{\epsilon}{\frac{1}{2}\overline{q^2}}(\overline{v^2}-\frac{1}{3}\overline{q^2})-\frac{1}{3}C_2\,\overline{uv}\left(h\frac{\partial U}{\partial n}+5\frac{U}{R}\right)$
$\frac{1}{2}\overline{w^2}$	$\frac{D}{Dt}(\frac{1}{2}\overline{w^2})$	$C_t\frac{\partial}{\partial n}\left(h\frac{\overline{q^2}}{2\epsilon}\overline{v^2}\frac{\partial\overline{w^2}}{\partial n}\right)$	—	$-\frac{1}{3}\epsilon$	$-C_1\frac{\epsilon}{\frac{1}{2}\overline{q^2}}(\overline{w^2}-\frac{1}{3}\overline{q^2})-\frac{1}{3}C_2\overline{uv}\left(h\frac{\partial U}{\partial n}-\frac{U}{R}\right)$
$\overline{uv}$	$\frac{D}{Dt}(\overline{uv})$	$C_th\frac{\partial}{\partial n}\left(\frac{\overline{q^2}}{2\epsilon}\overline{v^2}\frac{\partial\overline{uv}}{\partial n}\right)$	$-\overline{v^2}\left(h\frac{\partial U}{\partial n}-\frac{U}{R}\right)+2\left(\overline{u^2}-\overline{v^2}\right)\frac{U}{R}$	—	$-C_1\frac{\epsilon}{\frac{1}{2}\overline{q^2}}\overline{uv}+C_2\left[\overline{v^2}\left(h\frac{\partial U}{\partial n}-\frac{U}{R}\right)-2(\overline{u^2}-\overline{v^2})\frac{U}{R}\right]$
ϵ	$\frac{D\epsilon}{Dt}$	$C_\epsilon\frac{\partial}{\partial n}\left(h\frac{\overline{q^2}}{2\epsilon}\overline{v^2}\frac{\partial\epsilon}{\partial n}\right)$	$-C_{\epsilon1}\frac{\epsilon}{\frac{1}{2}\overline{q^2}}\left[\overline{uv}\left(h\frac{\partial U}{\partial n}-\frac{U}{R}\right)\right]$	$-C_{\epsilon2}\frac{\epsilon^2}{\frac{1}{2}\overline{q^2}}$	—

TABLE 1. Terms in the modelled transport equations for the Reynolds stresses and dissipation rate of turbulent energy. $C_t = 0{\cdot}22$, $C_1 = 1{\cdot}8$, $C_2 = 0{\cdot}6$, $C_\epsilon = 0{\cdot}18$, $C_{\epsilon1} = 1{\cdot}45$, $C_{\epsilon2} = 1{\cdot}90$, $h \equiv (1+n/R)$.

3. Calculation method

The modelled transport equations of the previous section are solved simultaneously with the momentum and continuity equations of the mean flow. For this to be done with reasonable economy of computer time a 'marching' solution is preferred to the complete 'elliptic' solution for which CB provide explicit boundary conditions. Consequently the curvature of the mixing layer is supplied as an input to the calculations and is not predicted. This restriction is quite acceptable since the sole objective of the study is to assess the performance of the turbulence model and the calculation of the flow field referred to fixed co-ordinate axes is irrelevant.

The s-direction momentum equation is (Bradshaw 1973)

$$\frac{DU}{Dt} = -\frac{1}{\rho}\frac{\partial p}{\partial s} - \frac{UV}{R} - \left[1+\frac{n}{R}\right]\frac{\partial \overline{uv}}{\partial n} - 2\frac{\overline{uv}}{R} - \left[\frac{\partial \overline{u^2}}{\partial s}\right], \tag{11}$$

in which the viscous diffusion terms have been omitted for high-Reynolds-number flow. The normal-stress gradient, shown in square brackets in (11) for completeness, is also not retained in the calculations. The neglected term has negligible influence on the development of the plane-mixing layer (it is ignored in the conventional thin-shear-layer approximation) and in the curved layer the pressure term dominates so that the net effect of the normal stress gradient on the total pressure on a given streamline is small. The continuity equation is

$$\frac{\partial U}{\partial s} + \frac{\partial}{\partial n}\left[\left(1+\frac{n}{R}\right)V\right] = 0 \tag{12}$$

and the equation set is completed by an abbreviated form (in which normal stress gradients are again omitted) of the n-direction momentum equation:

$$\left(1+\frac{n}{R}\right)\frac{1}{\rho}\frac{\partial p}{\partial n} = \frac{U^2}{R}. \tag{13}$$

Here again the Reynolds-stress gradients which would appear in the complete expression are dominated by the cross-stream pressure gradient so that this simple form adequately describes the pressure and mean-velocity fields (figures 1 and 2).

The radius of curvature, R, of the shear-flow centreline defined by CB, is taken from figure 2(b) of that paper where its reciprocal, K, is plotted against s. Initial conditions are required at the nozzle lip, $s = 0$; these are obtained as a result of preliminary calculations for a plane mixing layer and specified as those prevailing in a self-preserving flow of 3 mm thickness. The boundary conditions at the outer edge of the flow where the velocity is zero are simply that the pressure is equal to the atmospheric pressure and all the dependent variables are zero. At the high-velocity edge all the turbulence quantities are zero in the potential flow. The mean velocity, U, which is non-uniform at the edge of the solution domain, is required as a boundary condition for (11). The following approximate procedure is adopted: starting from an 'upstream' value of s at which all quantities are known, (13) is integrated across the layer to determine the static pressure at the high velocity edge. 'Upstream' values

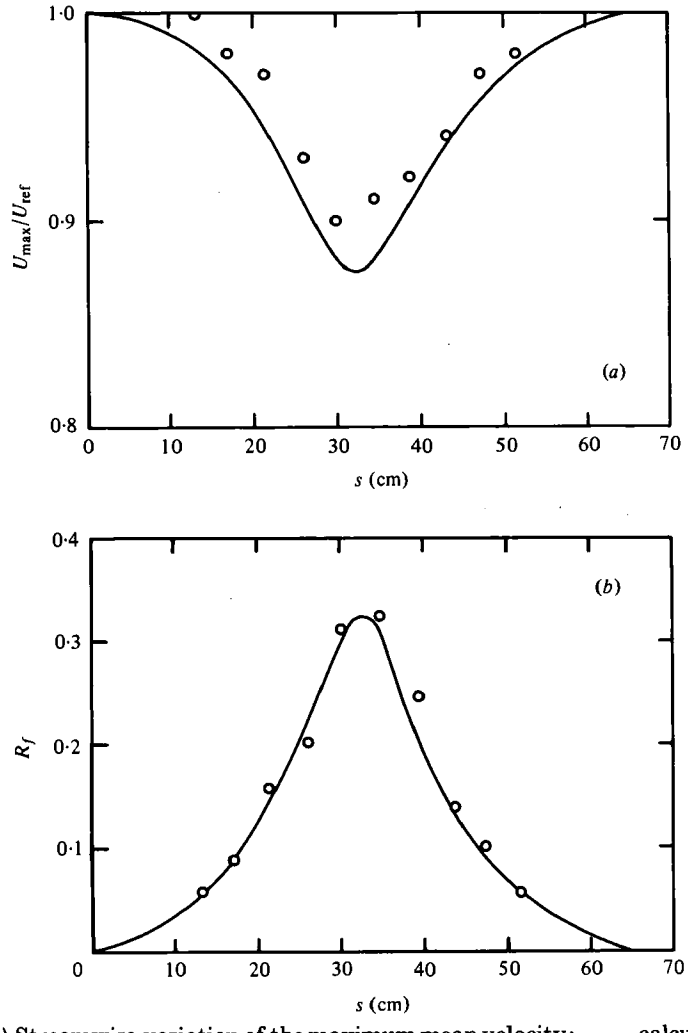

FIGURE 2. (*a*) Streamwise variation of the maximum mean velocity: ——, calculated; ○, measurements by Castro (1973). (*b*) Variation of the curvature Richardson number along the centreline.

of the streamwise pressure gradient are used to estimate the edge value of U at the downstream station, $s+\delta s$, from

$$U\frac{\partial U}{\partial s} = -\frac{1}{\rho}\frac{\partial p}{\partial s} \tag{14}$$

integrated along a streamline.

This fairly crude approximation can obviously be refined by, for example, successive iteration. Provided, however, that small forward steps in s are taken, the mean velocity in the potential flow is calculated to within 3%. Figure 2(*a*) shows the resulting streamwise variation of the maximum velocity which is chosen for this comparison because it is most readily identified in the experimental data; the normalizing velocity, U_{ref}, is the mean velocity in the nozzle exit plane. The solution domain extends some distance into the potential flow where the mean velocity decreases with increasing radius of curvature. A further partial check on the

correctness of the method is provided by a comparison of the measured and calculated variation of the curvature Richardson number along the centreline which is plotted in figure 2(*b*). This quantity is defined by:

$$R_f \equiv \frac{2\dfrac{U}{r}}{\left(\dfrac{\partial U}{\partial r}+\dfrac{U}{r}\right)} \tag{15}$$

in which $r(\simeq n+R)$ is the local streamline radius of curvature. R_f is interpreted as (minus) the ratio of $\overline{v^2}$ production (due to streamline curvature) to the total $\overline{u^2}$ production and it is analogous to the flux Richardson number of buoyant flow which is also defined as a ratio of energy production terms. Overall, the level of agreement shown in figure 2 justifies the approximate method for the pressure field and potential velocity.

A computer code based on the Patankar & Spalding (1970) GENMIX boundary-layer program is used. Numerical instabilities, which have appeared in the calculation of other complex flows (Launder & Morse 1979; Samaraweera 1978), and which necessitated the use of staggered grid arrangements, are entirely absent in this case. The forward step size, which for a plane flow and in the absence of strong longitudinal pressure gradients would be taken as about one tenth of the shear layer thickness, is limited by the procedure adopted to deal with (14). Approximately 700 forward steps are needed to obtain grid independent solutions and, with a cross-stream grid of thirty-three nodes, the computation time on a UNIVAC 1108 computer is approximately 0·6 s per step.

4. Comparison of model predictions with experiment

The results of calculations are now compared with the measurements reported by CB. Some experimental data are also taken from Castro (1973) which contains details of the plane mixing layer only briefly mentioned in CB. That this simple flow be adequately predicted appeared to be an essential prerequisite for calculating the curved layer, but the usefulness of the plane mixing layer as a standard for turbulence-model performance is, however, limited by the very considerable spread in the data reported from various sources. In reviewing these data Rodi (1975) concluded that the measurements of Bradshaw *et al.* (1964) in the initial region of a round jet showed the best internal consistency and these have therefore been included in table 2 with Castro's data and the results of the present calculations.

The mixing-layer thickness, δ, is defined by CB as the distance between the points where $(P-p_a)/\frac{1}{2}U_{\rm ref}^2$ takes the values 0·81 and 0·0625. P is the total pressure, p_a is the atmospheric pressure and $U_{\rm ref}$ is the jet velocity in the plane of the nozzle. For the plane-mixing layer, where the static pressure is negligibly different from p_a, these definitions give $U/U_{\rm ref} = 0{\cdot}9$, 0·25. The centre-line is defined as the line $U/U_{\rm ref} = 0{\cdot}67$.

Table 2 shows that the predicted rate of growth of the self-preserving plane mixing layer is 11 % less than Castro's measured value. The agreement between the measured and calculated velocity profiles, which are shown as the lowest pair of curves in figure 4, is somewhat less satisfactory. In fact, examination of the velocity profiles from different sources plotted by Rodi (1975) shows that Castro's results are atypical

Source	$\frac{d\delta}{dx}$	$\frac{\overline{q^2}}{U_{ref}^2}$	$\frac{\overline{u^2}}{U_{ref}^2}$	$\frac{\overline{v^2}}{U_{ref}^2}$	$\frac{\overline{w^2}}{U_{ref}^2}$	$\frac{\overline{uv}}{U_{ref}^2}$	$\frac{\overline{uv}_c}{U_{ref}^2}$
Bradshaw *et al.* (1964)	—	0·0570	0·0210	0·0170	0·0190	0·0100	0·0100
Castro (1973)	0·113	0·0557	0·0264	0·0131	0·0163	0·0085	0·0098
Present calculations	0·102	0·0542	0·0270	0·0136	0·0136	0·0096	—

TABLE 2. Comparison of calculated and measured values of spreading rate and maximum values of turbulent energy and Reynolds stress in self-preserving mixing layers. $\overline{uv}_c$ is the value of $\overline{uv}$ deduced from mean-flow measurements.

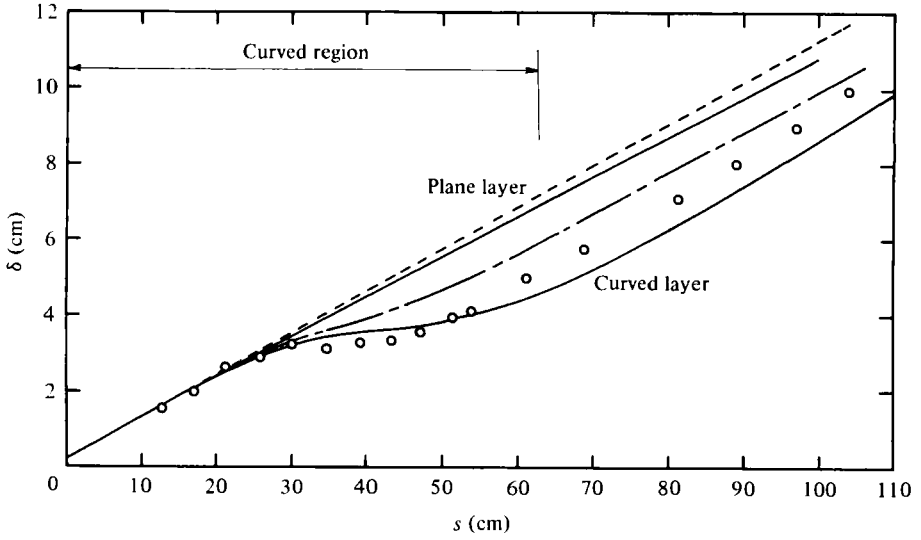

FIGURE 3. Calculated and measured values of the shear-layer thickness plotted against distance s measured along the centreline: ○, curved-layer data; – – –, plane-layer data; ——, Reynolds-stress model; —·—, k–ϵ model.

to an extent that accounts almost entirely for the discrepancy in U on the low-velocity side and for some of that on the high-velocity side. Some discrepancy at the high-velocity edge is not unexpected since it appears also in all previous calculations with turbulence models based on one or more transport equations. In this respect the present predictions differ only slightly from those of LRR and are close to a consensus of mean-field data.

The turbulent energies and Reynolds stresses shown in table 2 are the maximum values normalized by the square of the mean velocity at the edge of the layer. The maximum value of $\overline{q^2}$ is predicted to within 3 % of the measurements and the levels of the three components appear to be about right, although a minor defect of the pressure-strain model is that it always produces $\overline{v^2} = \overline{u^2}$ for a simple shear layer. The calculated shear stress is nearly equal to that measured by Bradshaw *et al.* and the values shown in the last column of table 2, which are obtained by Castro (1973) by substituting measured velocity distributions in the integral-momentum equation. The discrepancy between these and the directly-measured value led Castro to conclude that the latter is probably too low by 15–20 %. The shear stress obtained in the present calculations thus appears to be very nearly correct.

Attention is now turned to the curved mixing layer. Figure 3 shows calculated and

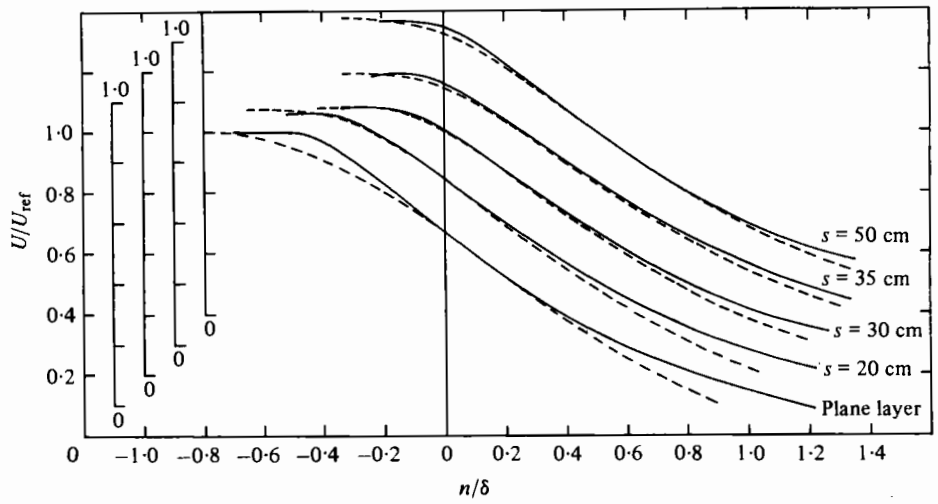

FIGURE 4. Profiles of mean velocity at different streamwise locations: ——, calculated; – – – –, faired curves through the measurements. Curves displaced upwards and to the right.

measured values of the layer thickness, δ, plotted against distance s measured along the centre-line. The spreading rate $d\delta/ds$ falls to very low values around the region of maximum curvature ($s \approx 33$ cm) but recovers in the vertical portion of the flow downstream ($s > 62$ cm) to a value slightly greater than that of the plane layer. The calculated layer growth corresponds to the measurements; the main points of difference are that the response to the extra strain and its removal is not quite as rapid as that measured. A further comparison made in figure 3 is with the layer growth calculated using a popular two-equation closure method† which gives good results for plane flow but does not adequately account for the effects of curvature.

The calculated profiles of mean velocity agree rather better with the measurements than in the plane-flow case, as is shown in figure 4 where the measured profiles are taken from the contour plots provided in CB. On the low-velocity side the calculated profiles show the same trends as for the plane-mixing layer and the velocity is consistently overpredicted. On the high-velocity side, however, the agreement is improved. It will be recalled that the edge velocity is calculated by integrating the cross-stream momentum equation (13) across the layer; the graphs show the decrease in U from a maximum value to that at the edge of the solution domain some distance into the potential flow.

In the remaining figures the calculated and measured effects of curvature on turbulence quantities are compared. Attention has already been drawn to the overshoot of plane-layer values which CB describe as the most striking feature of their results. Some overshoot appears also in the calculations; it is shown in figure 5 where the maximum values of $\overline{q^2}$ and $\overline{uv}$ are plotted against distance s measured along the

† In the $k-\epsilon$ turbulence model, (Launder & Spalding 1974) transport equations are solved for $k(\equiv 0{\cdot}5\overline{q^2})$ and ϵ. The shear stress is calculated from the gradient transport formula:

$$-\overline{uv} = 0{\cdot}09\,\frac{k^2}{\epsilon}\left[\left(1+\frac{n}{R}\right)\frac{\partial U}{\partial n}-\frac{U}{R}\right]$$

and curvature effects are introduced solely through the definition of $P(10)$.

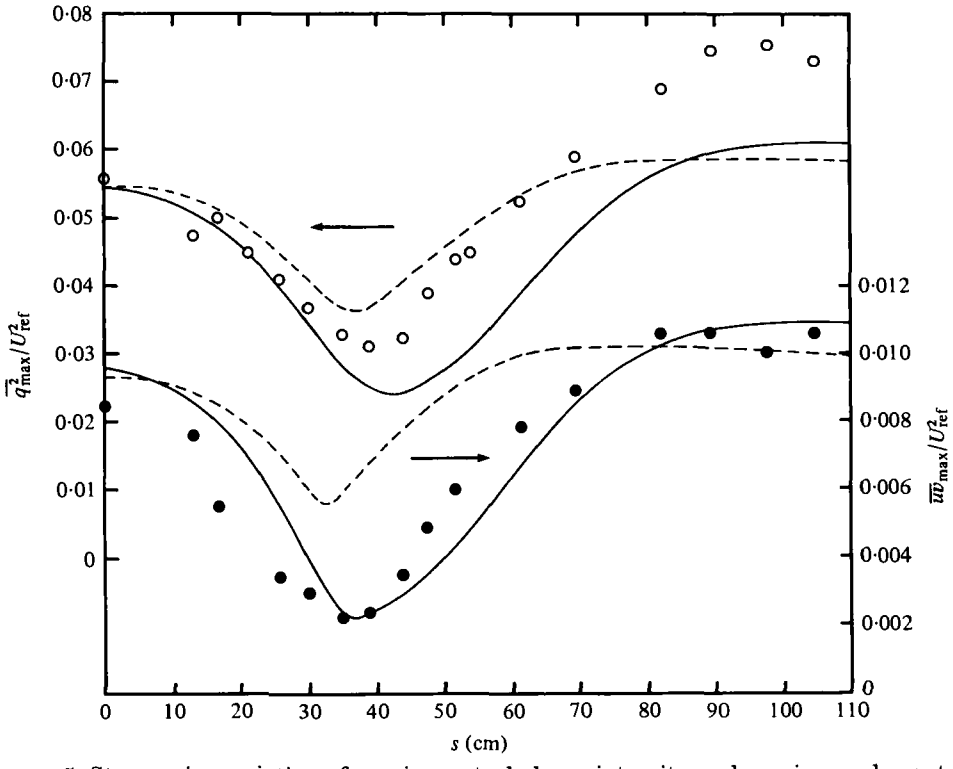

FIGURE 5. Streamwise variation of maximum turbulence intensity and maximum shear stress: ——, Reynolds stress model; – – – –, k–ϵ model; ○ measured $\overline{q^2}$; ● measured $\overline{uv}$.

centre-line. The model reproduces quite closely the sharp fall in intensity and shear stress to minimum values close to the point of greatest curvature. The calculated recovery of $\overline{q^2}$ is less rapid, and although the maximum value downstream exceeds that in a plane layer by 13 % this is to be compared with a 35 % measured overshoot. The calculated and measured overshoots in $\overline{uv}$ are in closer agreement at 18 and 25 % respectively. The calculated turbulent-energy production rate in the recovery zone is less than that reported in CB and this may account for some of the discrepancy in $\overline{q^2}$ However, since the streamwise variation of $\overline{u^2}_{max}$, shown in figure 6, is quite accurately predicted it seems probable that a low production rate is also associated with a low rate of intercomponent transfer due to pressure strain. The calculated behaviour of $\overline{v^2}_{max}$ (figure 6) appears to support this conjecture and the pressure-strain term in the shear-stress balance, shown in figure 9 and discussed below, is also underestimated. A feature of the measurements shown in figure 6 is that $\overline{u^2}_{max}$ and $\overline{v^2}_{max}$ both fall to 59 % of their plane-layer values. That $\overline{v^2}$ does not fall more than $\overline{u^2}$ is rather surprising since the direct effects of stabilizing curvature, expressed by the generation terms in the transport equations (1) and (2), are to augment $\overline{u^2}$ and to depress $\overline{v^2}$. Accordingly in the calculations $\overline{v^2}_{max}$ falls to 47 % and $\overline{u^2}_{max}$ falls to as little as 36 % of their plane-layer values.

It is instructive to compare the results for $\overline{uv}$ and $\overline{q^2}$ with the performance of the $k-\epsilon$ model which is also shown in figure 5. Here the streamwise variation of $\overline{q^2}$ is quite well predicted from the transport equation but the eddy-viscosity formulation fails badly to reproduce the observed fall in $\overline{uv}$.

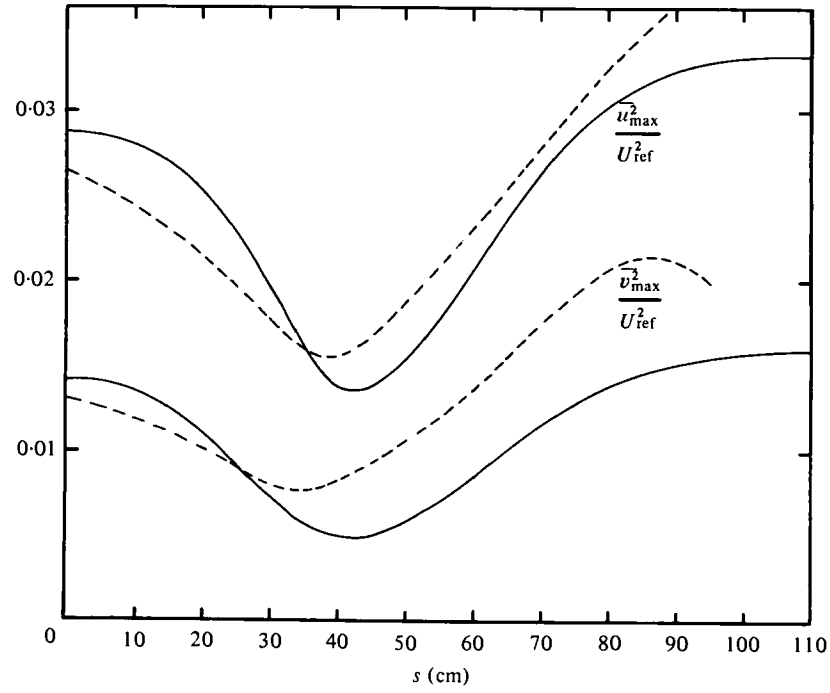

FIGURE 6. Streamwise variation of maximum values of the normal stresses: ——, calculated; – – – –, measured values obtained from contour plots presented by Castro & Bradshaw (1976).

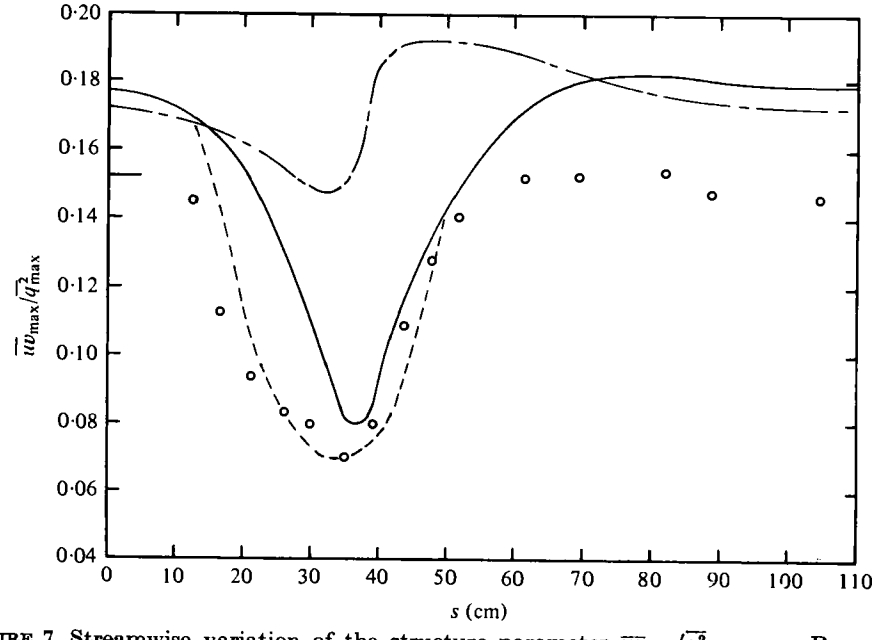

FIGURE 7. Streamwise variation of the structure parameter $\overline{uv}_{max}/\overline{q^2}_{max}$. ——, Reynolds-stress model; – – –, k–ϵ model; – – – –, rapid-distortion model (Townsend 1980); ○, CB data.

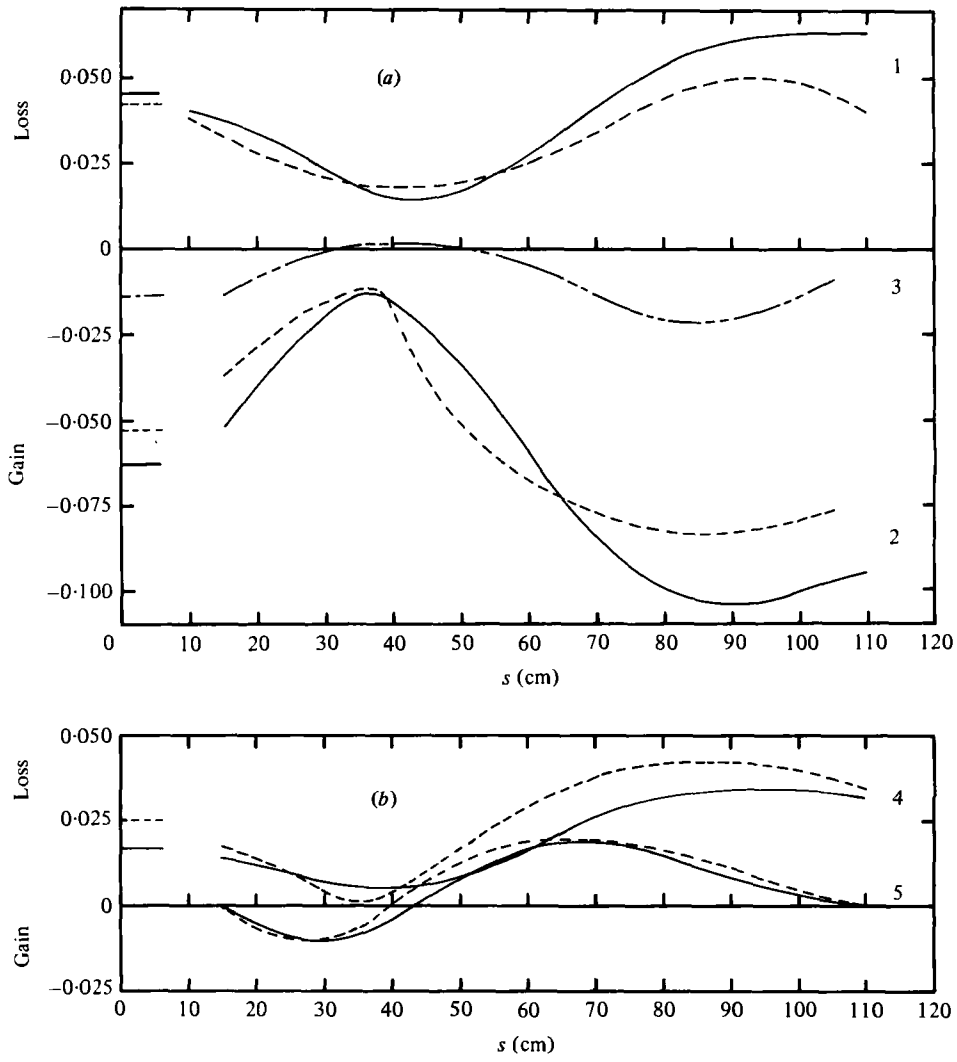

FIGURE 8. Terms in the turbulent energy equation on the centreline; all quantities made dimensionless by U_{ref}^3/s. Solid lines represent calculated values; broken lines are faired through the experimental data. Plane-layer values are shown on the ordinate. (*a*) 1, dissipation; 2, production; 3, out-of-balance term (measurements). (*b*) 4, turbulent transport; 5, advection.

As a consequence the observed fall and recovery in the structure parameter $\overline{uv}/\overline{q^2}$ is not predicted as is shown in figure 7. In fact the use of the eddy-viscosity formula with a constant coefficient (0·09) implies an approximately constant value for $\overline{uv}/\overline{q^2}$. The Reynolds-stress model does predict the fall of $\overline{uv}/\overline{q^2}$ to the right level although it overshoots the measured values downstream due mainly to the underprediction of $\overline{q^2}$ discussed above.

It is not easy to accept Townsend's (1980) view that the observed effects are 'not easily associated with source terms in the transport equation for Reynolds stress'. A local-equilibrium analysis (in which the source terms of table 1 are equated to zero) shows immediately that $\overline{uv}/\overline{q^2}$ is a strong function of the local curvature Richardson

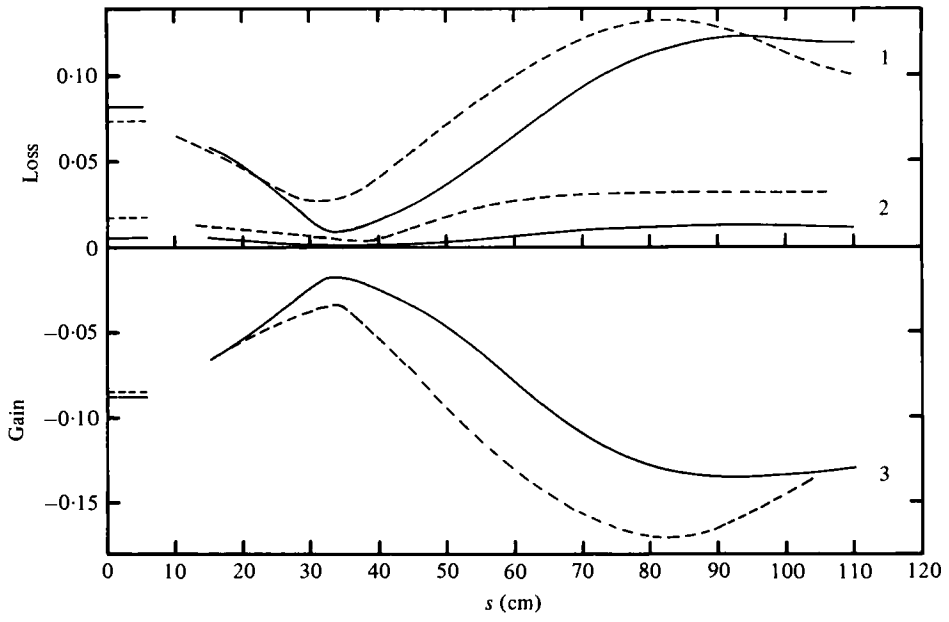

FIGURE 9. Terms in the shear-stress transport equation on the centreline; all quantities made dimensionless by U_{ref}^3/s. Solid lines represent calculated values; broken lines are faired through the experimental data. 1, pressure strain; 2, turbulent transport; 3, production. Plane-layer values are shown on the ordinate.

number†. Although Townsend (1980) finds it surprising that $\overline{uv}/\overline{q^2}$ should recover towards the plane-layer value before the curvature becomes negligible it is apparent from the modelled equations that this quantity must rise beyond the point of maximum curvature (at approximately 45°) as R_f starts to fall. The local equilibrium approximation does in fact reproduce this behaviour with fair accuracy. Townsend's results for $\overline{uv}/\overline{q^2}$ are also shown in figure 7 for comparison.

Terms in the turbulent-energy equation and the $\overline{uv}$ transport equation are compared with measured values on the centre-line in figures 8 and 9. Turbulent transport by pressure fluctuations was neglected by CB in processing the data and the main destruction term in the $\overline{uv}$ equation, the pressure-strain correlation, was obtained by difference. The 'out-of-balance' term plotted in figure 8(*a*) is attributed by CB to inaccuracy in the measurement of the dissipation rate, ϵ, from frequency spectra and not to neglect of pressure transport. For clarity in making the comparisons mean-flow transport of $\overline{uv}$, which is very small, has been omitted from figure 9 and the shear-stress generation terms presented separately by CB have been combined. The measured behaviour of the terms plotted in figures 8 and 9 is discussed at some length by CB. This discussion need not be repeated and it is enough to note that the calculated

† The result obtained by Gibson (1978) is

$$\frac{\overline{uv}}{\overline{q^2}} = \left[\beta(R_f)\,\frac{2-R_f\overline{v^2}}{1-R_f\overline{q^2}}\right]^{\frac{1}{2}}$$

where $\beta(R_f)$ is the eddy-viscosity coefficient whose value for plane flow is determined by the model constants.

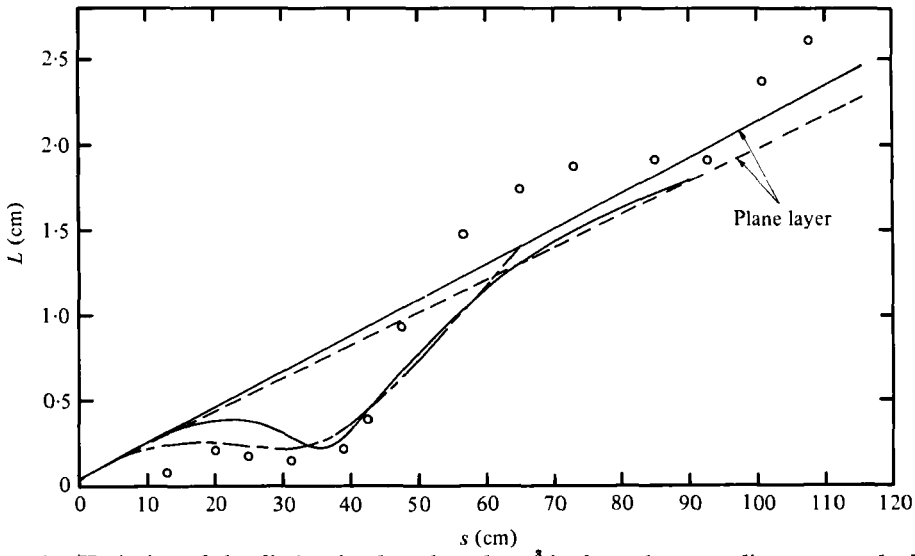

FIGURE 10. Variation of the dissipation length scale $\overline{uv}^{\frac{3}{2}}/\epsilon$ along the centreline. ——, calculated; ○, curved-layer data; – – – –, plane-layer data; –·–·–·–, $L = L_0(1+7R_f)^{-1}$.

behaviour is in broad accord with that measured, the agreement being rather better in the energy balance than in the $\overline{uv}$-equation terms. CB ascribe the steep rise in $\overline{q^2}$ and $\overline{uv}$ as the curvature decreases to a rapid increase in the rate of shear strain leading to increases in the production terms. The reason why the increase is prolonged is attributed by CB to the suppression of turbulent transport which permits an unusual increase in turbulent energy in the central part of the layer. Figure 8(*b*) shows that the calculated increase in turbulent diffusion in the region of decreasing curvature is smaller than that measured and it might therefore be expected that the calculated rise and overshoot of $\overline{q^2}$ would exceed the measured values. In the calculated balance, however, the sluggish response of the triple correlations approximated by (8) is more than offset by a less rapid rise in energy production.

A feature of the results is that the turbulent-energy dissipation rate obtained from the modelled transport equation (9) corresponds fairly closely to the measured values, even when the out-of-balance term in the measurements is taken into account. The ϵ-equation is widely used in turbulence modelling but, while it produces acceptable results for many simple shear flows, its performance in more complex flows has recently been questioned (Launder & Morse 1979; Hanjalic & Launder 1979). For the curved shear layer the basic form originally proposed by Hanjalic & Launder (1972) appears to be quite adequate, with the single (logical) change that turbulent energy production due to mean shear in a simple flow is replaced by the total (shear plus curvature) production.

Figure 10 shows measured and calculated values of the dissipation length scale $L \equiv \overline{uv}^{\frac{3}{2}}/\epsilon$ on the centre-line. The calculated variation of L with s shows a minimum of about the right value at $s = 36$ cm but the steep measured rise and overshoot of plane-layer values is not recovered. The main reason for the discrepancy is the slow calculated response of $\overline{uv}$ to the reduction in curvature, although high calculated

values of ϵ downstream also contribute. CB comment that the curvature is changing too rapidly for validity of a 'Monin–Obukhov' linear correction factor of the form:

$$L/L_0 = (1+\beta R_f)^{-1}, \tag{16}$$

where β is a constant (Bradshaw 1969). The calculated values cannot be fitted by (16) either, although the difference is not as great as that measured. The length scale variation obtained from (16) with $\beta = 7$ is plotted in figure 10 for comparison. We have verified that the use of (16) in place of the ϵ equation (9) does in fact produce an overshoot in turbulence quantities although the overall level of agreement with the measurements is poorer. It appears then that the ability to predict this feature depends not on the use of a length scale equation or its equivalent, but is a consequence of the characteristics of the other transport equations. Smits *et al.* (1979) have arrived at the same conclusion by using a crude stress transport model to show that the response of a turbulent shear layer to a perturbation is a damped oscillatory variation in $\partial U/\partial n$ and $\overline{uv}$. Townsend (1980), appealing to rapid-distortion theory, also interprets the shear-stress behaviour as being the consequence of damped inertial waves that can propagate in flows with stabilizing curvature. CB report similar behaviour of the length scale $L_\epsilon \equiv (\overline{q^2})^{\frac{3}{2}}/\epsilon$ which is not recovered at all in the calculations. The only effect of curvature on the calculated values of L_ϵ is slightly to diminish its rate of increase with s. The variation is not, however, simply related to the layer thickness or to the local values of R_f.

5. Concluding remarks

The present study has demonstrated that a calculation method based on the Reynolds-stress equations reproduces the main features of a turbulent shear layer subjected to strong stabilizing curvature. These consist of the reduction in growth rate relative to a plane flow, the suppression of turbulent intensity and shear stress in the highly-curved region, the subsequent recovery to, and overshoot of, plane-layer values downstream of the curved zone. The availability of very detailed turbulence measurements has made possible comparisons that are seldom attempted in model studies of this type, including such details as the balances of turbulent energy and shear stress.

The Reynolds-stress model is one which had previously been developed for plane flow. The effects of strong curvature are predicted without modification to the basic closure hypotheses, or changes in the model constants whose values are established in advance by reference to experimental data from simple shear layers. In the interests of retaining a model which, it is hoped, will be generally applicable to practical flow calculation, no attempt has been made to 'tune' the model constants for optimum agreement with either plane or curved mixing-layer measurements. The predictions compare favourably with results obtained from a 'standard' unmodified lower-order model in which empirical curvature corrections are certainly needed to achieve the same level of agreement with the measurements.

In his paper describing rapid-distortion calculations for this flow, which result in the streamwise variation of $\overline{uv}/\overline{q^2}$ reproduced in figure 7, Townsend (1980) suggests that calculation schemes based on the Reynolds-stress equations cannot give correct

results. The present work does not support Townsend's views and a short discussion of the two approaches is appropriate.

The Reynolds-stress equations are exact and, while it is necessary to model certain terms to close the equation set, the closure approximations used are based on physical reasoning and satisfy symmetry and continuity conditions. The model for the pressure-strain correlation is the central feature of the closure scheme. This quantity is decomposed into two parts which are modelled separately. The model for the mean-strain, or 'rapid', part is not incompatible with rapid-distortion theory and indeed the two methods reduce to the same exact result for the case of initially isotropic turbulence subjected to weak distortion. The treatment differs from that advocated by Townsend in that the local mean strain ($\partial U/\partial n - U/R$) is used throughout rather than an 'effective total strain'.

In the CB flow the change in distortion over distances comparable with the integral scale is slight enough to permit the local strain to be used in the Reynolds-stress model. The history of the flow, and thus also the history of the strain, is accounted for by the transport terms in the equations albeit not in the model for the mean-strain part of the pressure-strain correlation. It is, perhaps, worth emphasizing again that the Reynolds-stress closure is complete and that the method gives absolute values of turbulence quantities which are required for the simultaneous calculation of the mean-flow field.

In its current form the rapid-distortion model is restricted to the prediction of stress ratios in flows where the mean-flow details are supplied rather than predicted. If it were to form part of a calculation scheme at least one additional equation would be needed to determine intensities. The method is based on a local linearization of the equations of motion. The interaction of large stable eddies with mean-flow gradients is modelled while the nonlinear interactions with other eddies are assumed to be weak. In relation to the terms of the exact Reynolds-stress equations the method implies neglect of turbulent transport (triple correlations), the turbulence part of pressure strain and the energy-dissipation rate†. Consequently the rapid-distortion theory is strictly applicable only when the turbulence is weak and the distortion time is small compared to a characteristic decay time for the turbulence. Since, however, only the stress ratios are calculated the restriction is not too severe. The shear-stress transport equation in particular is dominated by the mean-flow distortion terms and equivalent results can be obtained from a local-equilibrium approximation to the full equations. In any case it appears that the assumptions made for each model are not seriously violated, that is, the distortion is neither extremely rapid nor very slow. There seems to be no insuperable difficulty involved in reconciling the essential features of both methods. Such an approach, which has already been suggested by Hunt (1978), might well afford the best prospect for development of a generally applicable calculation method for complex flows.

We gratefully acknowledge the support provided for this research by the Deutsche Forschungsgemeinschaft while one of the authors (MMG) was a visitor to the Sonderforschungsbereich 80 at the University of Karlsruhe. The calculations were performed on the UNIVAC 1108 computer of the University of Karlsruhe. Our thanks

† Inter-eddy transfer, and thus dissipation, are however accounted for in Townsend's (1980) scheme by an eddy-viscosity approximation.

are due also to Professor P. Bradshaw and Dr I. P. Castro for reading and providing helpful comments on an earlier version of the manuscript.

REFERENCES

BRADSHAW, P., FERRISS, D. H. & JOHNSON, R. F. 1964 Turbulence in the noise-producing region of a circular jet. *J. Fluid Mech.* **19**, 591–624.

BRADSHAW, P. 1969 The analogy between streamline curvature and buoyancy in turbulent shear flow. *J. Fluid Mech.* **36**, 177–191.

BRADSHAW, P. 1973 Effects of streamline curvature on turbulent flow. *AGARDograph* 169.

CASTRO, I. P. 1973 A highly distorted turbulent free shear layer. Ph.D. thesis, Imperial College, London.

CASTRO, I. P. & BRADSHAW, P. 1976 The turbulence structure of a highly curved mixing layer. *J. Fluid Mech.* **73**, 265–304.

DALY, B. J. & HARLOW, F. H. 1970 Transport equations in turbulence. *Phys. Fluids* **13**, 2634–2649.

GIBSON, M. M. 1978 An algebraic stress and heat-flux model for turbulent shear flow with streamline curvature. *Int. J. Heat Mass Transfer* **21**, 1609–1617.

GIBSON, M. M. & LAUNDER, B. E. 1976 On the calculation of horizontal, turbulent, free shear flows under gravitational influence. *Trans. A.S.M.E.* C, *J. Heat Transfer* **98**, 81–87.

GIBSON, M. M. & LAUNDER, B. E. 1978 Ground effects on pressure fluctuations in the atmospheric boundary layer. *J. Fluid Mech.* **86**, 491–511.

HANJALIC, K. & LAUNDER, B. E. 1972 A Reynolds-stress model of turbulence and its application to thin-shear layers. *J. Fluid Mech.* **52**, 609–638.

HANJALIC, K. & LAUNDER, B. E. 1979 Preferential spectral transport by irrotational straining. Paper at ASME Symposium on Turbulent Boundary Layers, Niagara Falls, New York.

HUNT, J. C. R. 1978 A review of the theory of rapidly distorted turbulent flows and its applications. *Fluid Dynamics Trans.* **9**, 121–152.

IRWIN, H. P. A. H. & SMITH, P. A. 1975 Prediction of the effect of streamline curvature on turbulence. *Phys. Fluids* **18**, 624–630.

LAUNDER, B. E. & MORSE, A. 1979 Numerical prediction of axisymmetric free shear flows with a second-order Reynolds-stress closure. Proc. 1st Symp. on Turbulent Shear Flow, Springer-Verlag, Heidelberg.

LAUNDER, B. E., REECE, G. J. & RODI, W. 1975 Progress in the development of a Reynolds-stress turbulence closure. *J. Fluid Mech.* **68**, 537–566.

LAUNDER, B. E. & SPALDING, D. B. 1974 The numerical computation of turbulent flows. *Computer Methods in Appl Mech. and Eng.* **3**, 269–289.

LESLIE, D. C. 1980 Analysis of a strongly sheared, nearly homogeneous turbulent shear flow. *J. Fluid Mech.* **98**, 435–448.

LUMLEY, J. L. 1980 Second order modelling of turbulent flows. In *Prediction Methods for Turbulent Flows* (ed. W. Kollmann). Hemisphere.

MELLOR, G. L. 1975 A comparative study of curved flow and density-stratified flow. *J. Atmos. Sci.* **32**, 1278–1282.

MORSE, A. 1979 Axisymmetric turbulent shear flows with and without swirl. Ph.D. thesis, University of London.

NAOT, D., SHAVIT, A. & WOLFSHTEIN, M. 1970 Interaction between components of the turbulent velocity correlation tensor. *Israel J. Tech.* **8**, 259.

PATANKAR, S. V. & SPALDING, D. B. 1970 Heat and Mass Transfer in Boundary Layers. Intertext Books.

REYNOLDS, W. C. 1970 Computation of turbulent flows: state-of-the-art. Rep. MD-27, Mech. Eng. Dept., Stanford University.

RODI, W. 1975 A review of experimental data of uniform density free turbulent boundary layers. Studies in Convection 1. Ed. B. E. Launder. Academic Press.

ROTTA, J. C. 1951. Statistische theorie nichthomogener turbulenz. *Z. Phys.* **129**, 547–572.

SAMARAWEERA, D. S. A. 1978 Turbulent heat transport in two- and three-dimensional temperature fields. Ph.D. thesis, Imperial College, London.

SMITS, A. J., YOUNG, S. T. B. & BRADSHAW, P. 1979 The effect of short regions of high surface curvature on turbulent boundary layers. *J. Fluid Mech.* **94**, 209–242.

TOWNSEND, A. A. 1980 The response of sheared turbulence to additional distortion. *J. Fluid Mech.* **98**, 171–191.

WYNGAARD, J. C., TENNEKES, H., LUMLEY, J. L. & MARGOLIS, D. P. 1968 Structure of turbulence in a curved mixing layer. *Phys. Fluids* **11**, 1251–1253.